SCIENTIFIC REPORTS

OPEN

SUBJECT AREAS:
SPINTRONICS
ELECTRONIC DEVICES
SURFACE SPECTROSCOPY
MOLECULAR ELECTRONICS

Received
11 January 2013

Accepted
11 January 2013

Published
15 February 2013

Correspondence and requests for materials should be addressed to M.B. (bowen@unistra.fr)

Direct observation of a highly spin-polarized organic spinterface at room temperature

F. Djeghloul[1], F. Ibrahim[1], M. Cantoni[2], M. Bowen[1], L. Joly[1,3], S. Boukari[1], P. Ohresser[4], F. Bertran[4], P. Le Fèvre[4], P. Thakur[5], F. Scheurer[1], T. Miyamachi[6], R. Mattana[7], P. Seneor[7], A. Jaafar[1], C. Rinaldi[2], S. Javaid[1], J. Arabski[1], J. -P Kappler[1], W. Wulfhekel[6], N. B. Brookes[5], R. Bertacco[2], A. Taleb-Ibrahimi[4], M. Alouani[1], E. Beaurepaire[1] & W. Weber[1]

[1]IPCMS UMR FSOH CNRS-UdS, 23 rue du Loess BP 43 67034 Strasbourg, France, [2]LNESS – Dipartimento di Fisica, Politecnico di Milano, Via Anzani 42, 22100 Como, Italy, [3]Swiss Light Source, Paul Scherrer Institut, 5232 Villigen PSI, Switzerland, [4]Synchrotron Soleil, L'Orme des Merisiers Saint-Aubin - BP 48 91192 Gif-sur-Yvette Cedex, France, [5]European Synchrotron Radiation Facility (ESRF), 38043 Grenoble Cedex, France, [6]Physikalisches Institut and Center for Functional Nanostructures, Karlsruhe Institute of Technology, Wolfgang-Gaede-Strasse 1, 76131 Karlsruhe, Germany, [7]Unité Mixte de Physique CNRS/Thales, 91767 Palaiseau, France associée à l'Université de Paris-Sud, 91405 Orsay, France.

Organic semiconductors constitute promising candidates toward large-scale electronic circuits that are entirely spintronics-driven. Toward this goal, tunneling magnetoresistance values above 300% at low temperature suggested the presence of highly spin-polarized device interfaces. However, such spinterfaces have not been observed directly, let alone at room temperature. Thanks to experiments and theory on the model spinterface between phthalocyanine molecules and a Co single crystal surface, we clearly evidence a highly efficient spinterface. Spin-polarised direct and inverse photoemission experiments reveal a high degree of spin polarisation at room temperature at this interface. We measured a magnetic moment on the molecule's nitrogen π orbitals, which substantiates an ab-initio theoretical description of highly spin-polarised charge conduction across the interface due to differing spinterface formation mechanisms in each spin channel. We propose, through this example, a recipe to engineer simple organic-inorganic interfaces with remarkable spintronic properties that can endure well above room temperature.

Technological progress in the past decade has been nothing short of astounding as revealed by our maturing information society. An important milestone will be to design not only electrical components but entire circuits that pervasively utilize the electron spin as well as its charge. In this vein, research has focused on the interface between ferromagnets (FM), whose current is spin-polarised, and organic semiconductors (OS), which have been identified as a promising medium to transport spin-encoded information due to low spin-orbit induced spin decoherence in this class of semiconductors[1]. A proof-of-concept experiment involving electrons far from the Fermi level E_F was recently reported[2].

When integrated into devices, such interfaces can yield large values of magnetoresistance at low temperature due to transport at/near E_F, whether in the diffusive regime[3], in the ballistic regime across individual molecules[4] or in the tunneling regime[5]. As supported by a phenomenological model, this latter result could underscore how, due to molecular chemisorption onto a transition metal surface, the OS's molecules at the interface may exhibit a molecular orbital (MO) at E_F[6] that extends the electrode conduction onto the first molecular monolayer(ML)[7]. Due to exchange-split bands, the unequal density of states (DOS) of the two spin populations at E_F in the FM is then believed to lead to a spin-selective broadening of this MO[5], i.e. to a spin-polarised interface[7] that is termed a spinterface[8]. This original mechanism of spinterface formation leads to band-induced spinterface states (BISS). Some of us have observed substantial (>500%), low-temperature tunneling magnetoresistance (TMR) across a fully organic barrier using Co/phthalocyanine (Co/Pc) interfaces. However, experiments have thus far not revealed large values of room temperature (RT) spin polarization (P) at/close to the Fermi level of such FM/OS interfaces, whether through spectroscopy techniques[9,10] or on actual devices[11]. In this sense, a validation of the promise behind the spinterface concept[5,8] --- namely more efficient interfaces for spintronic applications --- is still lacking. Indeed, the spinterface concept is a pre-requisite for ballistic[4], tunneling[5] and diffusive[3] regimes of

transport, while spin transport in the diffusive regime also requires spin conservation during transport across the OS bulk.

Results

In what follows, we demonstrate that solving this riddle requires the study of FM/OS interfaces whose structure and electronic properties are well characterised. Given the link between photoemission (PE) and magnetotransport spectroscopy techniques[12], we have performed spin-polarised direct and inverse PE experiments at RT on interfaces between fcc Co(001) and MnPc (see the molecular schematic in the inset to fig. 2e) or H_2Pc as potential spinterface candidates[4,7].

The PE experiments reveal the presence of Pc-induced states close to E_F[9,10]. In order to extract the signal coming only from the molecular sites, we adopt a subtraction procedure that takes into account the attenuation of the signal arising from ever deeper atomic sites away from the sample surface (see SI). We present in Fig. 1a the spin-resolved difference spectra of direct and inverse PE spectroscopy of Co/MnPc at RT (2.6 ML MnPc for direct and 2 ML MnPc for inverse PE) that are obtained by this subtraction procedure. Both direct and inverse PE experiments reveal significant (nearly no) spin ↑ (↓) intensity at/near E_F, which indicates a high P of the Pc-induced states in the vicinity of E_F. We note that very similar difference spectra (in direct PE) are also obtained in the case of H_2Pc, which shows that the central Mn^{2+}-ion in MnPc plays a minor role in the formation of the spinterface. Assuming that the spin asymmetry of spectra is directly related to P (see Ref. 11), we can safely state that the RT P at E_F of the first two layers of MnPc or H_2Pc adsorbed on Co(001) reaches +80% ± 10%, i.e. is opposite in sign to that of bare Co.

We now confirm the interfacial nature of P by examining the impact of additional Pc coverage. Upon appropriately subtracting the spin-resolved spectra of 1 ML H_2Pc/Co from those of 2 ML H_2Pc/Co, the intensity of the interface states is strongly reduced (see Fig. 1b): the second Pc layer contributes only 20% to the total intensity of the interface states of Fig. 1(a), which could reflect deviations from perfect layer-by-layer growth. The third ML does not contribute at all to the interface states' intensity. We have also excluded the artefact of an altered Co interface magnetism on our analysis and conclusions (see SI).

To determine whether these interface states originate dominantly from the Co substrate or the Pc-overlayer, we compared data for photon energies of 20 eV and 100 eV (see Fig. 1c). From 20 eV to 100 eV, the cross section of photoionisation for free atoms decreases by over one order of magnitude for 2*p* states (C and N) while that for 3*d* states (Co and Mn) does not vary much[13]. We expect that such a large effect for free atoms shall trend similarly in solid-state systems. Consequently, if the interface states were mainly of Co 3*d* character, they should also be present at 100 eV photon energy. However, the spin-resolved direct PE difference spectra at 100 eV show no indication for any Pc-induced structure at low binding energies. We thus conclude that the interface states are mainly of C or N 2*p* character.

Why does the interface between fcc Co(001) and MnPc or H_2Pc exhibit such a high P of PE at E_F, and this at RT? We propose the following key extension to the spinterface concept[5,8]: highly efficient, thermally robust spinterfaces may be engineered by choosing the ferromagnet/molecule pair such that the dominant interfacial hybridization mechanism involves states at/near E_F from the ferromagnet (FM) and molecule that are present only in one spin channel. In addition to the well-known spinterface formation mechanism of spin-dependent broadening in that spin channel[4,5,8], this promotes the hybridization in the other spin channel between the FM's surface states at the vicinity of E_F and MOs of the molecule. This mechanism ensures that energetically narrow and strongly spin-polarized hybrid interface states are pinned close to the Fermi level so as to drive the interface's spintronic response. The resilience of the ensuing spinterface properties against thermal disorder are enhanced not only by a large FM Curie temperature but also when direct exchange coupling that results from the hybridization mechanism magnetises at least some of the molecule's atoms.

When considering all electronic orbitals, ab-initio calculations on Co/Pc interfaces with unrelaxed atomic positions predicted a P that can reach -25%[7], rather than the +80% now measured experimentally. To more realistically describe the interface, our formalism now relaxes atomic positions and includes van der Waals forces so as to quantitatively reproduce the crucially important molecule-substrate distance inferred from x-ray standing wave measurements. This

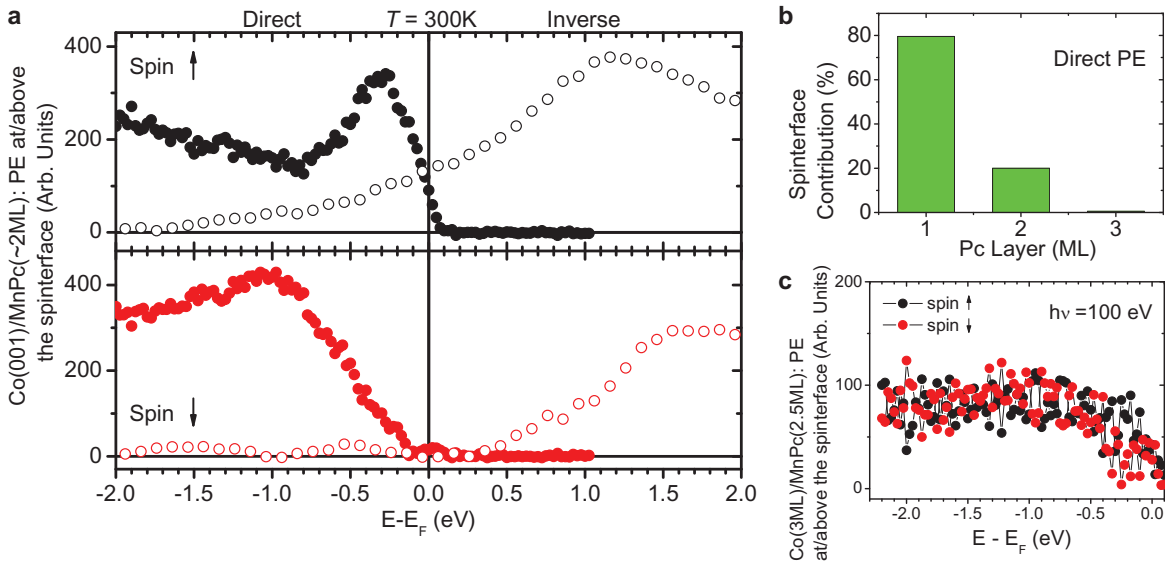

Figure 1 | Direct and inverse photoemission reveals a high interface spin polarisation P using commonplace Co and phthalocyanine molecules. (a) Spin-resolved difference spectra of direct (closed symbols; hν = 20 eV) and inverse (open symbols) photoemission (PE) spectroscopy at room temperature of Co/MnPc(2.6(2.0) ML for direct(inverse) PE) reveal a P∼+80% at E_F. (b) The Pc thickness dependence of the direct PE signal (hν = 20 eV) reveals that Pc-induced intensity at low binding energies is essentially confined to the interface. (c) Spin-resolved difference spectra of direct PE spectroscopy at room temperature of Co(3 ML)/MnPc(2.6 ML) for hν = 100 eV show no sign of any Pc-induced interface state, indicating that the interface states are mainly of C or N 2*p* character.

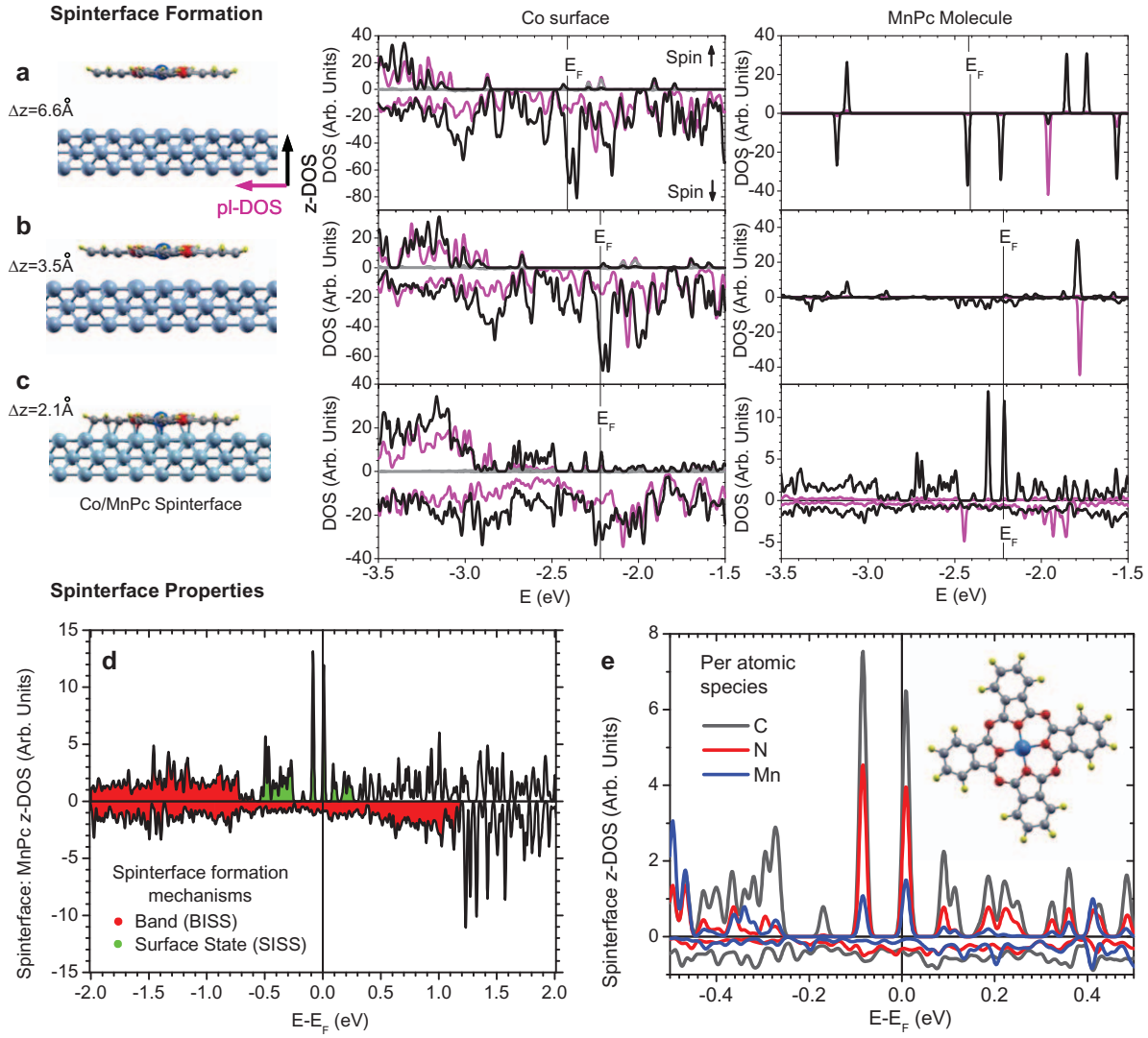

Figure 2 | The formation and properties of the Co/MnPc spinterface reflect distinct mechanisms in each spin channel. As the distance between molecule and the Co surface is reduced from (a) 6.6 Å to (b) 3.5 Å and to (c) the final position of 2.1 Å, *p-d* hybridization with the Co spin ↓ band causes energetically sharp, spin ↓ MOs in the z-DOS to disperse (red area of panel d), leading to a monotonous spin-↓ z-DOS (black) at/near E_F (right-hand graph of panel c). In the spin ↑ channel at the vicinity of E_F, there are neither Co *d* band states nor MOs but simply Co surface states (panel a) that begin to hybridize as the molecule is brought closer in (panel b) and lead, at the final molecular position (panel c), to energetically sharp peaks that cross E_F. These surface-induced spinterface states (SISS) carry virtually no Co s-character (gray datasets in panels a,b,c) and involve all atomic species of the molecule (panel e). The spinterface's planar DOS (pl-DOS; magenta) near E_F is mostly featureless and adopts the spin polarization of Co (right- and left-hand graphs of panel c).

leads to a final distance Δz between Co and the adsorbed molecule of 2.1Å.

To unravel the formation of the spinterface, we first consider the 'molecule-Co' system as calculated using the actual atomic positions of the final interface, but we artificially impose Δz = 6.6 Å. We can then examine the states of the two systems using a common Fermi level in the absence of interactions between them (see Fig. 2a). We extrapolated the spin referentials found for finite exchange coupling at lower Δz to those in the present case, at Δz = 6.6 Å, of vanishing exchange interactions between the two subsystems. The Co d- spin ↓ band crosses E_F, while the d spin ↑ band ends at $E-E_F = -0.7$ eV. Above this energy level, the spin ↑ sub-band exhibits only small DOS spikes that correspond to surface states. We note in particular one surface state at E_F with a strong perpendicular component (z-DOS, black) compared to its planar counterpart (pl-DOS, magenta). We emphasize that these surface states also exhibit a *s*-component of DOS (gray). Near E_F, the molecule exhibits a MO only in the spin ↓ channel. Adsorption-induced displacements of the molecule's atoms overall promote a slight energy shift (~30 meV) of the MOs.

We now turn on interactions between the molecule and the Co surface by reducing Δz to 3.5 Å (fig. 2b). At this distance, π orbitals that spatially extend perpendicularly to the nascent interface promote wavefunction overlap between the molecule and Co surface sites, causing E_F to shift from $E = -2.4$ eV to $E = -2.2$ eV. At the vicinity of E_F, the Co spin ↓ states and spin ↑ surface states are little affected. In contrast, the interaction strongly modifies the molecule's states: while planar states remain mostly unaffected, perpendicular states experience the onset of hybridization. In particular, this results in the energy dispersion of the initially sharp spin ↓ states in Fig. 2a at −2.4 eV and −2.2 eV. We emphasize here that there are no spin ↑ MO at/near E_F at Δz = 3.5 Å (right-hand panel of fig. 2b).

At the final Δz = 2.1 Å (fig. 2c), the molecule and Co surface sites may fully hybridize to form the spinterface. More precisely, all combinations of *s-p*, *p-d* and *s-d* hybridization may occur. Although fcc Co(001) has, near E_F, no *p* states and a highly spin-polarized *d* band, the flat, spin-degenerate *s*-band that crosses E_F is essentially responsible, through *s-d* hybridization[14], for the only moderate 45% spin polarization of conduction electrons. Yet, referring to Fig. 2c, the

spinterface formation involves Co *s*-states (gray datasets) only very weakly. Thus, although fcc Co(001) is obviously not half-metallic[15,16], the Co/MnPc spinterface shall strongly transmit the highly spin-polarized *d*-component of the Co DOS and attenuate the *s* and *p* components.

How is the Co *d*-band DOS transmitted onto the molecule in each spin channel? Prior to adsorption and in the spin ↓ channel, the Co *d* band z-DOS intersects E_F and the z-DOS of the free molecule also exhibits a MO at/near E_F. Hybridization is therefore governed by the well-known spinterface mechanism of spin-dependent broadening of MOs due to band hybridisation[4,5,8]. The resulting BISS (band-induced spinterface states) are shaded in red in fig. 2d. These BISS exhibit a flat, continuous energy dependence across E_F.

However, the molecule does not exhibit any sizeable, preexisting spin ↑ z-DOS at the vicinity of E_F to hybridise with, and the Co surface's *d*-band doesn't cross E_F. Another spinterface formation mechanism must therefore account for the appearance of entirely new, hybrid states in the spin ↑ channel within $-2.7\ eV < E < -1.9\ eV$, i.e. at the vicinity of E_F, (see right-hand panel of Fig. 2c and the segment of the spinterface z-DOS shaded in green in fig. 2d). We propose that preexisting Co surface states (see left-hand panel of Fig. 2a and b) pin initially distant MOs to E_F. The narrow energy width of these surface-induced spinterface states (SISS) reflects that of both the preexisting Co surface states --- because the surface atoms are missing bonds --- and of the preexisting MOs. Due to the Pauli exclusion principle, these newly formed SISS cannot occupy the spin ↓ states since they are already occupied by Co, and hence appear only in the spin ↑ channel. The presence of two sharp, tall peaks near E_F reflects a lifting of degeneracy induced by upward (downward) buckling of the benzene rings below(at) E_F along each of the two orthogonal axes that define the free molecule's 4-fold symmetry. This underscores how crucial it is to fully relax the interface structure if one wishes to study SISS.

Since surface states naturally lie at the vicinity of E_F, so shall SISS. Although SISS may appear as energetically sharp DOS peaks, which could reflect localization, SISS contribute to conduction across the interface. Indeed, the spectral signature of the SISS appears in the spin ↑ z-DOS of both Co surface and molecular sites (compare graphs of fig. 2c or refer to the SI). Focusing now on the DOS that contributes to transport at RT, we present in Fig. 3c–d spin-polarised spatial maps, taken along the dashed line of Fig. 3a, of the Co/MnPc interface DOS within $E_F - 25\ meV < E < E_F + 25\ meV$ (see Fig. 3b). Aside from the central Mn site, the remaining N and C sites exhibit very large positive P at E_F thanks to electronic states that are clearly hybridised with the Co interface atoms. In fact, these interface states are present on all atomic species of the molecule (fig. 2e) and their amplitude trends with the number of molecular nearest-neighbours for a given Co spinterface site.

At E_F, both the energetically smooth BISS in the spin ↓ channel and the energetically sharp SISS in the spin ↑ channel define the sign and amplitude of the spinterface's P. Due in large part to the energetically sharp SISS that crosses E_F, we find that P = 80%. Thus, considering the limitations of the comparison, we find that both theory and the direct/inverse PE experiments yield the same sign and high amplitude of P at E_F (see fig. 1a and 2e). Furthermore, peaks in the spin ↑ (↓) PE (see fig. 1a) and DOS spectra (see fig. 2d) at $\sim E - E_F = -0.3(-1.0)$ eV underscore a reasonably good agreement between theory and the direct PE experiment thanks to its good energy resolution (130 meV), while a qualitative agreement is found with inverse PE.

Since both PE experiments and ab-initio theory describe how the molecule's sites are spin-polarised, we now consider the magnetic properties of the spinterface. Referring to the on-site local magnetisation density map of Fig. 4a, our theory indicates that a strong antiferromagnetic (AF) coupling between Co and the numerous C benzene sites leads to a total magnetic moment for all C atoms of $-0.22\ \mu_B$. Within a Hund's rule description, this is expected since the Co *d* orbitals are more than half-filled. Only the partially filled *d* ↓ band may then hybridize, so that the coupling between C and Co is mediated essentially by minority electrons. Direct *p-d* coupling then leads to an exchange splitting of the C majority and minority DOS that is opposite in direction to that of Co.

The magnetic coupling of N sites is more subtle. Indeed, although N is coupled AF to Mn for free MnPc, molecular adsorption onto Co leads, through *d-d* hybridization, to ferromagnetic (F) coupling between Mn and Co (as expected since the Mn *d* band is less than

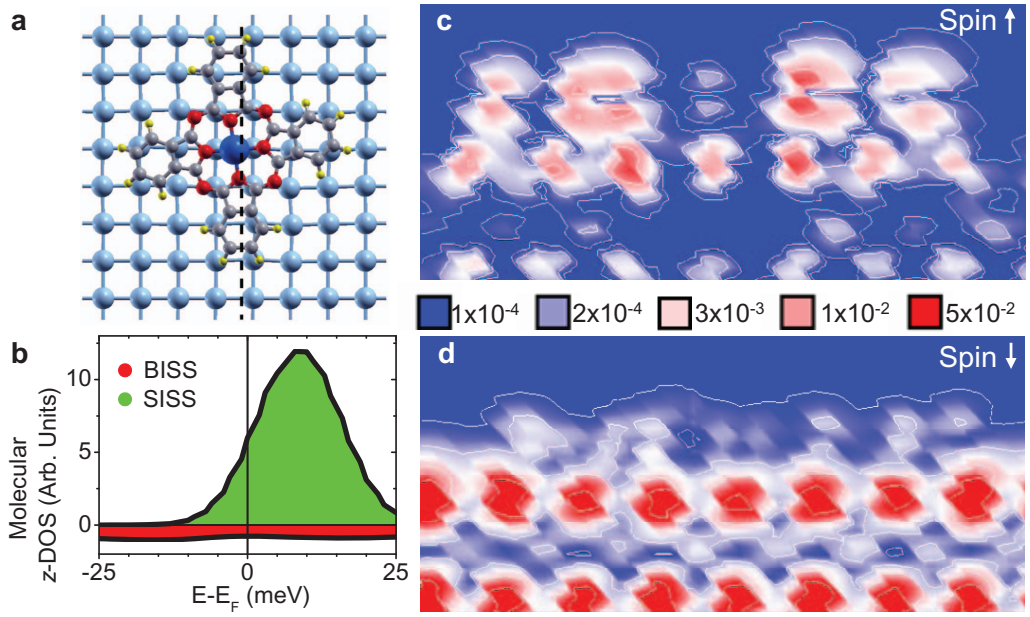

Figure 3 | The Co/MnPc spinterface as a highly spin-polarised current source. (a) Adsorption geometry of MnPc on Co(001). The spin ↑ and ↓ z-DOS within $E_F - 25\ meV < E < E_F + 25\ meV$: (b) SISS (BISS) lead to a sharp (monotonous) energy dependence at E_F; and (c–d) spatial charge density maps, taken along the dashed line of panel (a), show how the numerous C and N sites of MnPc exhibit a highly spin-polarised density of states at E_F that, furthermore, are hybridised with Co states and thus contribute to conduction. The maps are in umirs of e. $Å^{-3}$.

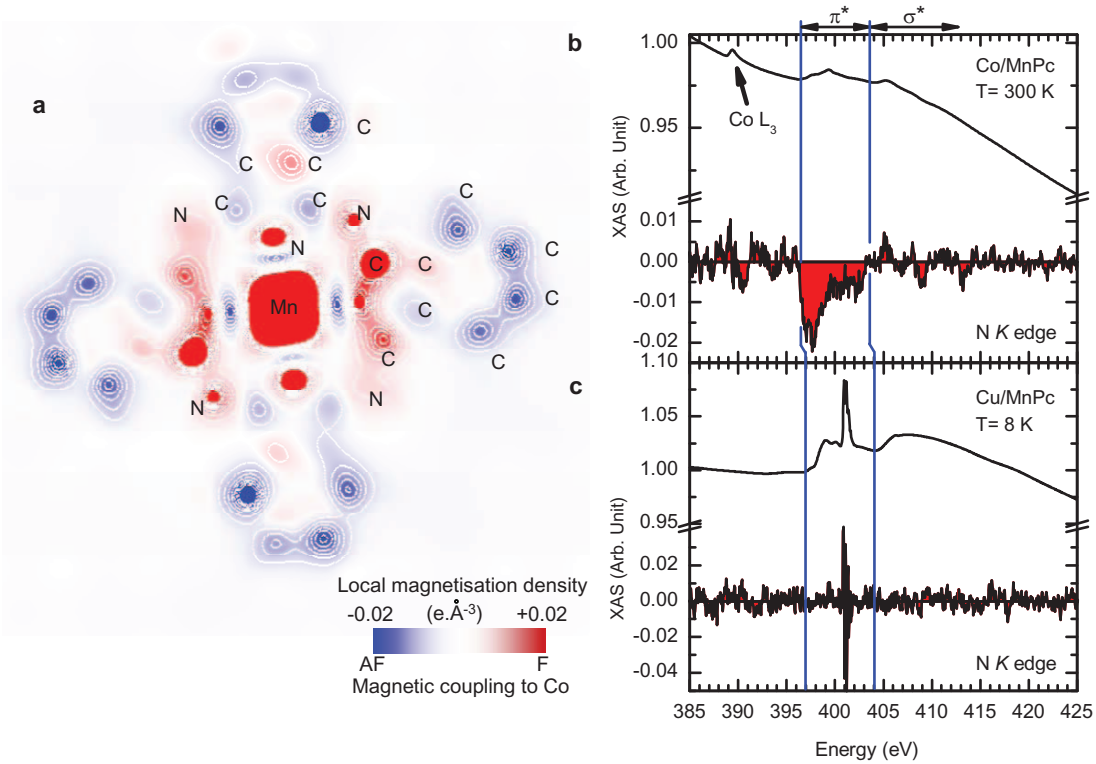

Figure 4 | Magnetic moments induced through direct exchange onto the molecular sites provide a signature of the Co/MnPc spinterface. (a) Top view of the on-site magnetisation density of the MnPc molecule adsorbed onto Co. While the pyrrole cage around Mn is ferromagnetically coupled to Co (F, red), that of the C-based benzene rings is mostly coupled antiferromagnetically (AF, blue) to Co. x-ray magnetic circular dichroic spectra acquired for H = 5 T and a 45° angle of photon incidence to the sample surface reveal a magnetic polarisation of the N π states of MnPc for (b) Co/MnPc(0.5 ML) at T = 300 K but not (c) Cu/MnPc(1.2 ML) even at T = 8 K. This confirms that the z-DOS of N just above E_F is spin-polarised. The slight energy shift of the N edge onset when going from Cu to Co reflects an increase in chemisorption strength[6].

half filled)[7,17]. Due to aromaticity, this F coupling is found to drive F coupling onto all N and C pyrrole sites. Thus, although C and N sites both contribute to the high P at E_F, their magnetisations are in fact opposite to one another.

If the molecule z-DOS is spin-polarized at E_F owing to BISS and SISS, then the molecule's π DOS at E_F should be spin-polarised. To support this theoretical description of spinterface magnetism, and as a tenet of spintronically active interfaces[18], we have performed x-ray magnetic circular dichroism (XMCD) experiments at the N *K* edge of MnPc's 8 nitrogen sites (see Methods). Referring to Fig. 4b, we witness XMCD intensity within the energy range corresponding to final 2p π (i.e. that probe the z-DOS just above E_F), but not 2p σ, states[7]. This unequivocal XMCD signal is very strong compared to the stray XMCD signal obtained when MnPc is adsorbed onto Cu(001) (see Fig. 4c), for which one does not expect the presence of on-site magnetic moments. The sharp absorption peak at 401 eV in the Cu/MnPc spectrum, which leads to the derivative-like XMCD signal, is in fact due to low-temperature N_2 adsorption. Since these are *K* edge transitions, we can only state[19] that an orbital magnetic moment appears on the final N 2p π states at the Co/MnPc spinterface, the sign of which is in agreement with that found theoretically. This experimentally confirms that the N z-DOS is spin-polarised as we have described theoretically.

Discussion

We now discuss spintronics prospects for these Co/Pc spinterfaces. Indeed, an ideal spin-polarized current source (IspCS) should 1) exhibit a very high degree of spin polarisation P that 2) endures well above RT for technological applications; 3) be both cheap and straightforward to synthesize considering existing industrial capabilities; 4) be compatible with miniaturisation challenges at the nanoscale; and 5) provide an easy integration path with a semiconductor so as to enable transport of, and operations on, the highly spin-polarised current. Behind criterion 5 lies the original promise of the spintronics field to promote the rise of an electronics in which not only individual electronic components (e.g. read heads in hard disks) but entire electronic circuits are conceived so as to encode and transport information using the electron spin.

Candidates toward an IspCS include half-metallic ferromagnets, which ideally conduct electrons of only one spin direction[15] and could, using merely a band hybridisation mechanism of spinterface formation[5,8], lead to efficient spinterfaces. Such materials have been studied using direct PE[20] and been integrated into devices with sizeable P, not only at low temperature[16] but also at RT[21]. However, this track fails criteria 3 and 4 for an IspCS because such materials are sensitive to disorder. Dilute magnetic semiconductors offer an interesting solution to criterion 5, but lose their half-metallic property well below RT[22]. Another track is to resistively filter the current so as to spin-polarise it. Fe/MgO-based IspCS accomplish this[23] through tunneling across MgO[24] and can reach P = 85%[25], but this resistive solution to spin-filtering a) must involve several dielectric monolayers that b) must be of finite lateral extent in order to promote $k_{//}$ conservation. This resistive solution is therefore not as practical toward nanoscale applications (criterion 4) as a conductive one involving merely an interface that can scale down laterally to the individual molecule[4].

In contrast, the Co/Pc interface involves differing spinterface formation mechanism in each spin channel to yield a high P (criterion 1). Since both mechanisms are driven by direct rather than indirect[17] hybridisation, the resulting current source is spin-filtered across a conductive[6,7] interface (criterion 4) and inherits the large temperature resiliency of the Co interface magnetisation

(criterion 2). Such spinterfaces utilize cheap, abundant materials that can be straightforwardly deposited and will not degrade when processed appropriately into devices[26] even at typically large process temperatures[27] (criterion 3). Finally, with its spin-polarized molecular plane, this IspCS candidate elegantly mitigates[9] the conductivity mismatch problem[28] associated with interfaces between metals and semiconductors, which is promising toward satisfying criterion 5, at the very least when considering a Pc OS. Indeed, the hybridization of wavefunctions from the interfacial molecular plane of high P with those of subsequent molecular layers away from the interface is intrinsically favored. Furthermore, referring to Fig. 3, conductivity is substantially lowered when going from Co to the Pc spinterface due to a strongly attenuated spin ↓ channel. These attributes of the Co/Pc spinterface represent important pre-requisites toward a future room-temperature demonstration of sizeable spin transport in the diffusive regime.

In conclusion, using direct and inverse PE, we have explicitly measured the interface contribution to the spin polarized DOS for Pc monolayers on Co(001), the so-called spinterface. At room temperature, the spinterface around the Fermi level is strongly dominated by the majority channel, leading to a spin polarization P∼80%. Thus, our work on Co/Pc interfaces provides a direct proof of the promise behind the spinterface concept, which was initially described in terms of band-induced spinterface states (BISS)[5,8]. We propose to extend this concept to include the additional spinterface formation mechanism of surface-induced spinterface states (SISS). SISS appear if the FM band of the dominant hybridisation mechanism is absent near E_F in one spin channel. This criterion is for example satisfied in the spin ↑ channel by strong ferromagnets such as Co or Ni. By combining BISS and SISS in separate spin channels, the spintronic response of these spinterfaces is not only large but can potentially be controlled through external stimuli. For example, due to the adsorbed molecule's lower symmetry, we find that rotating the magnetisation by 90° shifts the SISS peak at E_F by ∼1 meV, leading to a 10% change in P. Underscoring this effect is the spinterface's magnetic anisotropy, which can itself in principle be controlled using an electric field (e.g. Ref. 29) so as to more substantially alter the spinterface properties.

Finally, these spinterfaces constitute a strong candidate toward satisfying the five criteria for an IspCS, so as to pervasively use the electron spin, not simply in individual electronic components, but in future electronics industrial designs. Indeed, the P amplitude that we extract from spectroscopy experiments at RT and from theory is in agreement with that inferred from low-temperature TMR experiments across Co/Pc/Co nanojunctions. Thus, our results lay out a materials strategy for TMR devices with sizeable TMR at RT, as a stepping stone toward consequent spin transport in the diffusive regime at RT. Beyond future Co/Pc-based spintronic demonstrators based on the well-established tunneling mechanism of spin-polarized transport, we are presently working to extend these spinterface-induced IspCS concepts to memristive organic interfaces[30,31], so as to pave the way for robust organic multifunctional devices alongside their inorganic counterparts[32].

Methods

To prepare samples for x-ray absorption (XAS), spin-polarised photoemission (SPARPES) and spin-polarised inverse photoemission (SPIPES) experiments, we used a Cu(100) single crystal as substrate. It was cleaned by sputtering and annealing at 900 K. MnPc and H_2Pc were sublimated (P∼10^{-9} mbar, 1 monolayer (ML) = 0.38 nm) so as to form ultrathin films on Cu(100) or on Co(100) layers epitaxially grown on Cu(001). XAS were acquired (beamlines SIM at SLS and ID8 at ESRF) in total electron yield mode (P < 2×10^{-10} mbar) by reversing both the circular polarity of the photons and the sign of the external magnetic field. XAS were measured at the N K edge. The XMCD signal (ID8) was normalised to the height of the absorption edge step. The incidence angle was ∼45° to be sensitive to both in- and out-of-plane orbitals. We affirm a successful subtraction of the Co $L_{3,2}$ harmonics from the N K edge XMCD. Indeed, the N K edge XMCD is of same sign as the remnant Co L_3 harmonic. Since the Co L_3 and L_2 harmonics are necessarily of opposite sign, the measured XMCD cannot arise from the Co L_2 harmonic. Note that beamline ID8 exhibits a strong C absorption within the background spectrum that precluded XAS/XMCD experiments at the C K edge.

SPARPES experiments were undertaken on the Cassiopee Beamline at Synchrotron Soleil using photons at 20 and 100 eV and with the horizontal electric field impinging upon the sample at 45°. Photoelectrons were then acquired along a direction normal to the sample surface. The energy resolution is 130 meV.

SPIPES experiments were performed using a collimated and transversely polarised electron beam with 25% polarisation, from a GaAs photocathode. The SPIPES spectra are taken in the isochromatic mode by collecting photons at a fixed photon energy of 9.3 eV, while varying the incident-beam energy[33]. The energy of the incident electrons was varied between 9 and 17 eV. Data were collected at room temperature and at normal incidence. The energy resolution is 750 meV.

All density functional theory (DFT) calculations were carried by means of the VASP package[34] and the generalized gradient approximation for exchange-correlation potential as parametrized by Perdew, Burke, and Ernzerhof[35]. We used the projector augmented wave (PAW) pseudopotentials as provided by VASP[36]. The van der Waals (vdW) weak interactions were computed within the so called GGA-D2 approach developed by Grimme[37] and later implemented in the VASP package[38]. Our formalism can correctly reproduce the experimentally determined atomic distances between molecular sites and metallic sites. Fcc Co(001) and fcc Cu(001) surfaces were modeled by using a supercell of 3 atomic monolayers of 8 × 8 atoms separated by a vacuum region. The lattice vector perpendicular to the surface is 3 nm. This results in a supercell of 249 atoms, including the 57 atoms of the MnPc molecule. Since experiments used cobalt epitaxially grown on Cu, we used the fcc lattice parameter of 0.36 nm for both cobalt and copper. We have found that additional monolayers will not change significantly the results[39]. A kinetic energy cutoff of 450 eV has been used for the plane-wave basis set. For our study of a single molecule on metallic surfaces, we used only the gamma point to sample the first Brillouin zone. DOS were calculated using a 1 meV energy mesh and a Gaussian broadening of 20 meV full-width at half-maximum. Spin-orbit coupling was included pertubatively in the augmentation region at each atomic site.

1. Dediu, V. A., Hueso, L. E., Bergenti, I. & Taliani, C. Spin routes in organic semiconductors. *Nature Mater.* **8**, 707–716 (2009).
2. Cinchetti, M. *et al.* Determination of spin injection and transport in a ferromagnet/organic semiconductor heterojunction by two-photon photoemission. *Nature Mater.* **8**, 115–119 (2009).
3. Xiong, Z. H., Wu, D., Vardeny, Z. V. & Shi, J. Giant magnetoresistance in organic spin-valves. *Nature* **427**, 821–824 (2004).
4. Schmaus, S. *et al.* Giant magnetoresistance through a single molecule. *Nature Nanotech.* **6**, 185–189 (2011).
5. Barraud, C. *et al.* Unravelling the role of the interface for spin injection into organic semiconductors. *Nature Phys.* **6**, 615–620 (2010).
6. Takács, A. F. *et al.* Electron transport through single phthalocyanine molecules studied using scanning tunneling microscopy. *Phys. Rev. B.* **78**, 233404 (2008).
7. Javaid, S. *et al.* Impact on Interface Spin Polarization of Molecular Bonding to Metallic Surfaces. *Phys. Rev. Lett.* **105**, 077201 (2010).
8. Sanvito, S. Molecular spintronics: The rise of spinterface science. *Nature Phys.* **6**, 562–564 (2010).
9. Lach, S. *et al.* Metal–Organic Hybrid Interface States of A Ferromagnet/Organic Semiconductor Hybrid Junction as Basis For Engineering Spin Injection in Organic Spintronics . *Adv. Funct. Mater.* **22**, 989–997 (2012).
10. Methfessel, T. *et al.* Spin scattering and spin-polarized hybrid interface states at a metal-organic interface. *Phys. Rev. B.* **84**, 224403 (2011).
11. Santos, T. S. *et al.* Room-Temperature Tunnel Magnetoresistance and Spin-Polarized Tunneling through an Organic Semiconductor Barrier. *Phys. Rev. Lett.* **98**, 016601 (2007).
12. Bowen, M. *et al.* Spin-polarized tunneling spectroscopy in tunnel junctions with half-metallic electrodes. *Phys. Rev. Lett.* **95**, 137203(2005).
13. Yeh, J. J. & Lindau, I. Atomic subshell photoionization cross sections and asymmetry Parameters: 1 < Z < 103. *At. Data.& Nucl. Data Tables* **32**, 1–155 (1985).
14. Stearns, M. B. Simple explanation of tunneling spin-polarization of Fe,Co,Ni and its alloys. *J. Magn. Magn. Mater.* **5**, 167 (1977).
15. Bowen, M. *et al.* Half-metallicity proven using fully spin-polarised tunnelling. *J. Phys. Condens. Matter* **17**, L407–L409 (2005).
16. Bowen, M. *et al.* Using half-metallic manganite interfaces to reveal insights into spintronics. *J. Phys. Condens. Matter.* **19**, 315208 (2007).
17. Wende, H. *et al.* Substrate-induced magnetic ordering and switching of iron porphyrin molecules. *Nature Mater.* **6**, 516–520 (2007).
18. Bowen, M. *et al.* Absence of induced moment in magnetic tunnel junction barriers. *Phys. Rev. B.* **73**, 012405 (2006).
19. Hippert, F. *et al.* Neutron and X-ray Spectroscopy: X-ray Magnetic Circular Dichroism by Baudelet, F. (Springer, 2005).
20. Park, J.-H. *et al.* Direct evidence for a half-metallic ferromagnet. *Nature* **392**, 794–796 (1998).
21. Tezuka, N., Ikeda, N., Mitsuhashi, F. & Sugimoto, S. Improved tunnel magnetoresistance of magnetic tunnel junctions with Heusler $Co_2FeAl_{0.5}Si_{0.5}$ electrodes fabricated by molecular beam epitaxy. *Appl. Phys. Lett.* **94**, 162504 (2009).

22. Dietl, T. A ten-year perspective on dilute magnetic semiconductors and oxides. *Nature Mater.* **9**, 965–974 (2010)
23. Bowen, M. *et al.* Large magnetoresistance in FeCo/MgO/Fe(001) epitaxial tunnel junctions on GaAs(001). *Appl. Phys. Lett.* **79**, 1655 (2001).
24. Butler, W. H., Zhang, X. -G., Schulthess, T. C. & MacLaren, J.M., Spin-dependent tunneling conductance of Fe|MgO|Fe sandwiches. *Phys. Rev. B* **63**, 054416 (2001).
25. Lee, Y. M., Hayakawa, J., Ikeda, S., Matsukura, F. & Ohno, H. Effect of electrode composition on the tunnel magnetoresistance of pseudo-spin-valve magnetic tunnel junction with a MgO tunnel barrier. *Appl. Phys. Lett.* **90**, 212507 (2007).
26. Szulczewski, G., Tokuc, H., Oguz, K. & Coey, J. M. D. Magnetoresistance in magnetic tunnel junctions with an organic barrier and an MgO spin filter. *Appl. Phys. Lett.* **95**, 202506 (2009).
27. Peisert, H. *et al.* Order on disorder: Copper phthalocyanine thin films on technical substrates. *J. Appl. Phys.* **90**, 466 (2001).
28. Schmidt, G., Ferrand, D. & Molenkamp, L. W. Fundamental obstacle for electrical spin injection from a ferromagnetic metal into a diffusive Semiconductor. *Phys. Rev. B.* **62**, R4790–R4793 (2000).
29. Shiota, Y. T. *et al.* Induction of coherent magnetization switching in a few atomic layers of FeCo using voltage pulses. *Nature Mater.* **11**, 39 (2012).
30. Miyamachi, T. *et al.* Robust Spin Crossover and Memristance across a Single Molecule. *Nature Commun.* **3**, 938 (2012).
31. Prezioso, M., *et al.* A Single-Device Universal Logic Gate Based on a Magnetically Enhanced Memristor, Adv. Mater. in press (2012).
32. Bowen, M. *et al.* Bias-crafted magnetic tunnel junctions with bi-stable spin-dependent states. *Appl. Phys. Lett.* **89**, 103517(2006).
33. Cantoni, M. & Bertacco, R. High efficiency apparatus for spin polarized inverse photoemission. *Rev. Sci. Instrum.* **75**, 2387 (2004).
34. Kresse, G. & Furthmuller J. Efficient iterative schemes for ab initio total-energy calculations using a plane-wave basis set. *Phys. Rev. B* **54**, 11169 (1996).
35. Perdew, J. P., Burke, K. & Ernzerhof M. Generalized Gradient Approximation Made Simple. *Phys. Rev. Lett.* **77**, 3865 (1996).
36. Kresse, G. & Joubert, D. From ultrasoft pseudopotentials to the projector augmented-wave method. *Phys. Rev. B* **59**, 1758 (1999).
37. Grimme, S. Semiempirical GGA-type density functional constructed with a long-range dispersion correction. *J. Comput. Chem.* **27**, 1787 (2006).
38. Bucko, T. *et al.* Improved description of the structure of molecular and layered crystals: Ab initio DFT calculations with van der Waals corrections. *J. Phys. Chem. A.* **114**, 11814 (2010).
39. Chen, X i. & Alouani M. Effect of metallic surfaces on the electronic structure, magnetism, and transport properties of Co-phthalocyanine molecules. *Phys. Rev. B* 82, 094443 (2010).

Acknowledgements

We thank the ESRF and SIM beamline staff for technical assistance. F. Djeghloul thanks ≪Le Ministère de l'enseignement Supérieur et de la Recherche Scientifique d'Algérie≫ (MESRS) for financial support. We acknowledge financial support from ANR PNANO grants ANR-06-NANO-053-01 and ANR-06-NANO-053-02, the EC Sixth Framework Program (NMP3-CT-2006-033370), the CNRS-PICS Program No. 5275, the Deutsche Forschungsgemeinschaft (DFG), the Center for Functional nanostructures (CFN), the International Center for Frontier Research in Chemistry and the French German University. S. Javaid thanks the Pakistani government (HEC) for financial support. This work was performed using HPC resources from GENCI-CINES Grant 2012-gem1100.

Author contributions

J.A. purified the molecules. W.We., R. B. and M.B. conceived the photoemission experiments. F.D., M.C., L.J., M.B., S.B., F.B., P.L., C.R., R.B., W.We. and A. T.-I. carried out the photoemission experiments. W.We., L.J., M.C., R.B., S.B., M.B. and E.B. analysed the data. M.B., S.B., E.B., F.S. and W.Wu. conceived the x-ray absorption experiments. S.B., L.J., S.B., P.O., P.T., F.S., M.B., R.M., T.M., S.J., J.-P. K. and E.B. carried out the experiments. S.B., P.O., F.S., M.B. and N.B. analysed the data. M.A. conceived the ab-initio theory along with M.B., S.B., E.B. and W.We. F.I., S.J. and A.J. carried out the calculations. F.I., M.B., M.A., S.B., W.We. and E.B. analysed the data. M.B. wrote the paper, assisted by F.I., W.We., M.A. S.B., E.B., W.Wu. and P.S. M.B. prepared final figures, assisted by W.We., M.C., F.I., P.O. and S.B. All authors discussed the results and commented on the manuscript.

Additional information

Supplementary information accompanies this paper at http://www.nature.com/scientificreports

Competing financial interests: The authors declare no competing financial interests.

How to cite this article: Djeghloul, F. *et al.* Direct observation of a highly spin-polarized organic spinterface at room temperature. *Sci. Rep.* **3**, 1272; DOI:10.1038/srep01272 (2013).